Supplement to: Cosmogenic ^{10}Be in pyroxene: laboratory progress, production rate systematics, and application of the ^{10}Be-^{3}He nuclide pair in the Antarctic Dry Valleys

Allie Balter-Kennedy[1,2], Joerg M. Schaefer[1,2], Roseanne Schwartz[1], Jennifer L. Lamp[1], Laura Penrose[1], Jennifer Middleton[1], Bouchaïb Tibari[3], Pierre-Henri Blard[3], Gisela Winckler[1,2], Alan J. Hidy[4], Greg Balco[5]

[1]Lamont-Doherty Earth Observatory, Columbia University, Palisades, NY, USA
[2]Department of Earth and Environmental Sciences, Columbia University, New York, NY, USA
[3]CRPG, CNRS, Université de Lorraine, 54 000 Nancy, France
[4]Lawrence Livermore National Laboratory, Livermore, CA USA
[5]Berkeley Geochronology Center, Berkeley CA USA

Correspondence to: Allie Balter-Kennedy (abalter@ldeo.columbia.edu)

S1. Redetermining surface sample locations and elevations

The six surface samples used in this work were originally collected in the early 1990s and described in publications by Schäfer et al. (1999) and Bruno et al. (1997). The publications did not include accurate latitude and longitude information, but rather the feature name and sample elevation (Table 1). Furthermore, it is likely that the elevations that were recorded using a pressure-based altimeter or early handheld GPS may not be accurate. In the absence of original field notebooks and photographs of the field sampling in the mid 1990s, we redetermined sample locations by comparing the reported elevations in Schäfer et al. (1999) to the U.S. Geological Survey topographic map of Taylor Glacier (1988), viewed in Quantarctica Version 3 (Matsuoka et al., 2021). Latitudes and longitudes were approximated by locating the reported elevation on the feature of interest (Table 1). These latitudes and longitudes are approximate, but the exposure ages, erosion rates and production rates presented in the main text are sensitive mainly to the elevation of the samples.

Elevations reported in Schäfer et al. (1999) for samples 446s (1530 m) and 464 (1515 m) collected from Mt. Insel are up to 120 m higher than the Mt. Insel summit elevation on the U.S. Geological Survey topographic map of Taylor Glacier (1988) of 1410 m (Table 1). To account for this discrepancy, we subtract 120 m from the elevations for those two samples reported in Schäfer et al. (1999) and use elevations of 1410 m and 1395 m for samples 446s and 464, respectively. The elevations reported in Schäfer et al. (1999) for samples 318, 439, NXP 93*52, and 444 can be located on their respective landscape features (Table 1); therefore, we have no reason to believe that major inaccuracies exist for those reported elevations.

As a sensitivity test, we quantify the effect of subtracting 120 m from all surface sample elevations under the assumption that all elevations reported in Schäfer et al. (1999) have 100-m-scale inaccuracies. Although the individual maximum and minimum values for $P_{10,sp,SLHL}$ increase by ~5–7% when lower elevations are implemented, the change in value for $P_{10,sp,SLHL}$ resulting from the exercise described in Sect. 5.1.3 of the main text is relatively minor, from 3.6 ± 0.2 to 3.7 ± 0.2 atoms g^{-1} yr^{-1}.

In summary, we perform our calculations in the main text using elevations for samples 446s and 464 that are 120 m lower than reported in Schäfer et al. (1999), based on the USGS topographic map of the region. There is no evidence that samples 318, 439, NXP 93*52, and 444 have inaccurate elevations in Schäfer et al. (1999), so we do not alter elevations for those samples in the calculations performed in the main text, although doing so by ~100 m would not affect our conclusions.

S2. Discrepancy in ^{3}He concentrations between labs

As shown in the main text, the ^{3}He concentrations in the CRPG-prepared samples are consistently ~15% lower than those prepared at BGC and LDEO. Photos of the CRPG-prepared samples reveal that some plagioclase may still have adhered to the pyroxene grains used for helium analysis (Fig. S1), which could explain the lower ^{3}He concentrations in the CRPG samples, as plagioclase does not quantitatively retain ^{3}He (Cerling, 1990). Neither the BGC nor CRPG samples were HF-leached, although the consistency between the CRONUS-P-normalized ^{3}He concentrations measured at BGC and LDEO suggests that the BGC pyroxenes were mostly free of plagioclase. To test the hypothesis that the CRPG-prepared LABCO samples contain feldspar, and the BGC LABCO samples do not, we estimate the mix of feldspar and pyroxene in those samples using major element data measured by ICP-OES (Tables S1, S2, and S6). In general, the predicted elemental composition of a sample is given as the weight percent of each mineral in the sample multiplied by the elemental composition of that mineral:

$$[\%E_{1,p} \quad \%E_{2,p} \quad \dots \quad \%E_{j,p}] = [\%m_1 \quad \%m_2 \quad \dots \quad \%m_i] \cdot \begin{bmatrix} \%E_{1,1} & \%E_{2,1} & \dots & \%E_{j,1} \\ \%E_{1,2} & \%E_{2,2} & \dots & \%E_{j,2} \\ \vdots & \vdots & \vdots & \vdots \\ \%E_{1,i} & \%E_{2,i} & \dots & \%E_{j,i} \end{bmatrix}$$

Here, $\%E_{j,p}$ is the predicted weight percent of a given element in a sample, $\%m_i$ is the weight percent of a given mineral within that sample, and $\%E_{j,i}$ is the weight percent of element j in a reference composition for mineral i. We assume that the CRPG-prepared and BGC-prepared samples are made up of some combination of pyroxene, feldspar, and magnetite. For feldspar, we use reference compositions of albite (Kracek and Neuvonen, 1952) and anorthite (Subramaniam, 1956) as endmembers. As a reference pyroxene composition, we use our ICP-OES measurements on the HF-etched LABCO pyroxenes, under the assumption that those are pure pyroxene and are representative of a typical Ferrar Dolerite pyroxene. The elements Fe, Al, Ca,

Na and Mg display the largest change across reference materials, so we use the weight percent of those elements in our calculation. We estimate the percentage of each mineral in the average CRPG- and BGC-prepared samples by minimizing the sum of squared offsets:

$$M = \sum_{j} (\left[\%E_{1,s}\ \%E_{2,s} \ldots \%E_{j,s}\right] - \left[\%E_{1,p}\ \%E_{2,p} \ldots \%E_{j,p}\right])^2$$

(Equation S1)

Where $\%E_{j,s}$ is the measured weight percent of each element in the sample and $\%E_{j,p}$ is the predicted weight percent of each element from Equation S1. We find that, given the elemental composition, the samples prepared at CRPG contain ~13% plagioclase (~7% albite and 6% anorthite) and 4% magnetite. Despite the similar ^{3}He concentrations among the BGC and LDEO samples, using the LDEO pyroxene composition in this fitting method for the BGC samples suggests they contain ~5% albite and 5% magnetite. Although plagioclase and magnetite are visible in the BGC pyroxenes as well (Fig. S1), the lack of an elevated Al concentration and the consistency with the LDEO ^{3}He concentrations suggests that contamination by ~5% plagioclase does not significantly alter the ^{3}He concentrations. Furthermore, the production rate of ^{3}He in magnetite is similar to that in pyroxene, and ^{3}He is quantitatively retained in magnetite, so the presence of small amounts of magnetite likely did not have a large effect on the ^{3}He concentrations. Nevertheless, the discrepancy in ^{3}He concentrations between labs confirms the need to carefully separate pyroxene grains for helium analysis, with HF leaching being the most efficient and complete way to remove adhering feldspars.

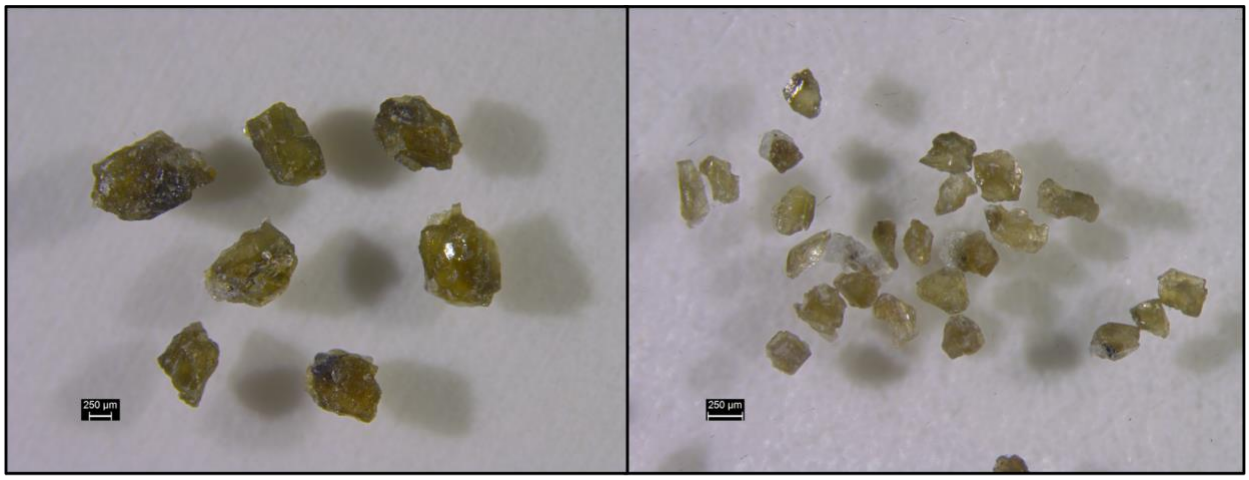

Figure S1: Pyroxene grains from CRPG-prepared sample DOL-17 (left) and BGC-prepared sample LABCO_155_157 (right). White minerals adhering to the grains are plagioclase, and darker opaque minerals are likely magnetite.

HF leaching of pyroxene grains also reduces the ^{4}He concentrations, raising the ^{3}He/^{4}He ratio (Bromley et al., 2014; Blard and Farley, 2008). The CRPG- and BGC-prepared samples have similar ^{4}He concentrations, while the ^{4}He concentrations in the LDEO-prepared samples are significantly lower (Fig. S2). Not only did we find the HF leaching efficient in removing meteoric ^{10}Be (see main text), but the comparison of ^{4}He concentrations among labs reiterates the value in HF leaching for increasing the ^{3}He/^{4}He ratio when making helium measurements.

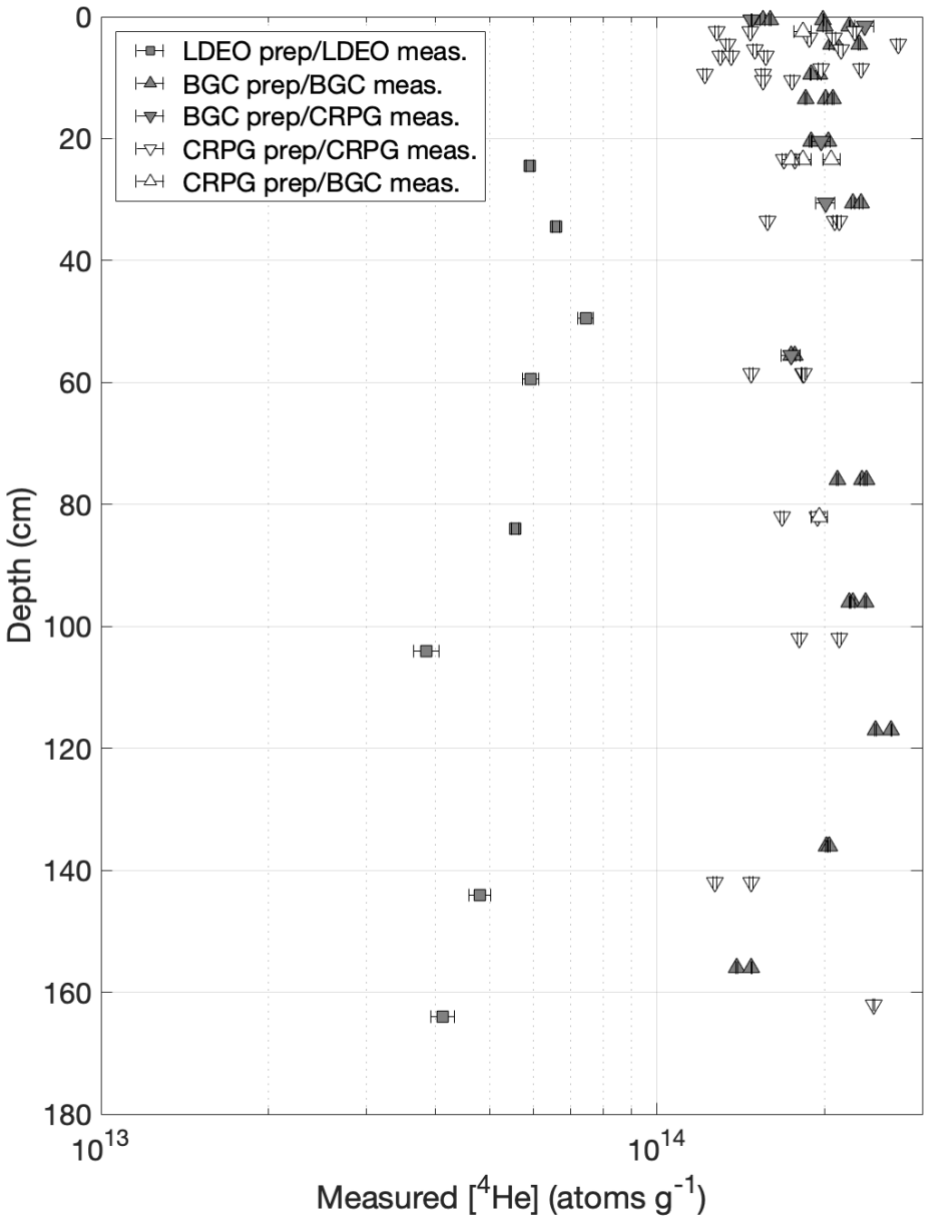

Figure S2: ^{4}He concentrations in LDEO-, BGC-, and CRPG-prepared pyroxene separates. The HF-leached LDEO-prepared samples are 40% lower than the BGC- and CRPG-prepared pyroxenes, which were not HF leached.

S3. Visual inspection of $Be(OH)_2$ precipitates

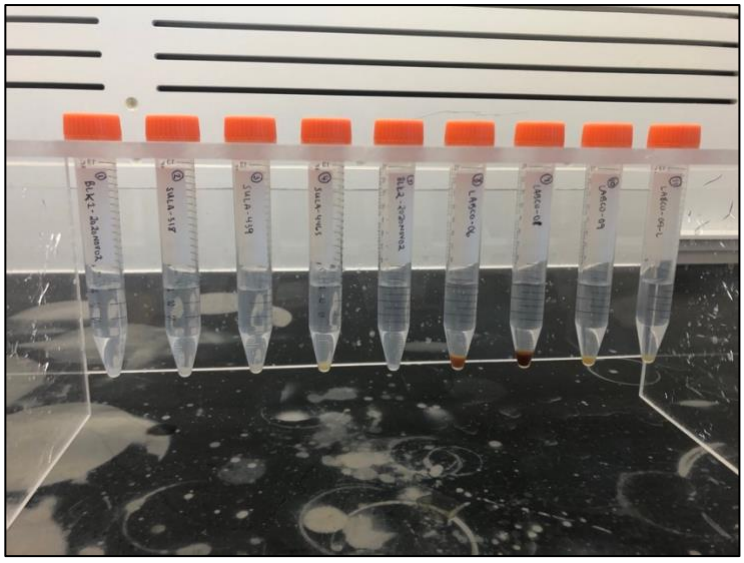

Figure S3 – Subset of $Be(OH)_2$ precipitates after the first round of cation exchange chromatography. As discussed in the main text, some samples exceeded the exchange capacity of the ion exchange resin, resulting in $Be(OH)_2$ precipitates noticeably larger than the blank. In this photo, the precipitates for samples LABCO-08 and -09 (3rd and 4th from right) are visibly larger than the blank (leftmost sample), prompting us to perform a second round of cation exchange chromatography. After the second round of cation exchange, all precipitates were visually similar in size to the blank.

S4. Quantifying ^3He production by fast muons

^3He measurements on pyroxene and ilmenite from the 300-m-long Cheney drill core from the Columbia River Basalt in Washington, USA provide unambiguous evidence for the production of ^3He by muons at a rate of 0.23–0.45 atoms g^{-1} yr^{-1} at sea-level high latitude (Larsen et al. 2021). Here, we use the ^3He measurements of Larsen et al. (2021) below 2000 g cm^{-2} depth to estimate the fast muon cross-section for ^3He and the concentration of nucleogenic ^3He present in the Columbia River Basalt. At these depths, the measured ^3He concentration includes ^3He produced by fast muons and nucleogenic ^3He:

$$N_{3,m} = N_{3,\mu f} + N_{3,nuc} \text{ (Equation S2)}$$

$N_{3,m}$ (atoms g^{-1}) is the measured ^{3}He concentration, $N_{3,\mu f}$ (atoms g^{-1}) is ^{3}He produced by fast muon reactions, and $N_{3,nuc}$ (atoms g^{-1}) is nucleogenic ^{3}He.

Production by fast muon interactions is taken from Heisinger et al. (2002a) as:

$$N_{3,\mu f} = \sigma_{0,3} N_{basalt} \int_0^t \beta(z)\phi(z)\bar{E}^{\alpha}(z)d\tau \quad \text{(Equation S3)}$$

Here, $\sigma_{0,3}$ is the cross-section for nuclide production by fast muons, N_{basalt} is the number of target atoms g^{-1} in standard basalt, assuming all elements are targets (2.74×10^{22} atoms g^{-1}; average atomic mass 22). We assume an exposure duration, t, of 16.6 Ma, which marks the onset of the Grande Ronde Basalt eruption (Kasbohm and Schoene, 2018). The remaining terms in these equations yield the integrated muon flux at a given mass depth over time for a surface erosion rate of zero (see Heisinger 2002a for symbol definitions). We evaluate Equation S2 with the "Model 1A" MATLAB code of Balco (2017), with the parameter α set to 1 (see discussion in Borchers et al., 2016; Balco 2017).

Equations S1 and S2 comprise a forward model that we use to predict ^{3}He concentrations below 2000 g cm^{-2} depth in the Cheney drill core. We fit our model by minimizing the χ^2 misfit statistic, M:

$$M = \sum_n \left[\frac{N_{3,p,n} - N_{3,m,n}}{\sigma_{3,m}^2} \right]^2$$

(Equation S4)

where $N_{3,p}$ is the predicted cosmogenic-nuclide concentration, $N_{3,m}$ is the measured cosmogenic-nuclide concentration, $\sigma_{3,m}$ is the associated measurement uncertainty. Following Larsen et al. (2021), all ^{3}He concentrations measured in ilmenite were converted into pyroxene equivalents

using a pyroxene/ilmenite production ratio of 0.78 (Larsen et al., 2019). The best-fitting values for the free parameters in the model are $\sigma_{0,3}$ = 6.01 μb and and $N_{3,nuc}$ = 5.87 x 10^6.

References

Balco, G.: Production rate calculations for cosmic-ray-muon-produced 10Be and 26Al benchmarked against geological calibration data, Quat Geochronol, 39, 150–173, https://doi.org/10.1016/j.quageo.2017.02.001, 2017.

Blard, P.-H. and Farley, K. A.: The influence of radiogenic 4He on cosmogenic 3He determinations in volcanic olivine and pyroxene, Earth Planet Sc Lett, 276, 20–29, https://doi.org/10.1016/j.epsl.2008.09.003, 2008.

Bromley, G. R. M., Winckler, G., Schaefer, J. M., Kaplan, M. R., Licht, K. J., and Hall, B. L.: Pyroxene separation by HF leaching and its impact on helium surface-exposure dating, Quat Geochronol, 23, 1–8, https://doi.org/10.1016/j.quageo.2014.04.003, 2014.

Bruno, L. A., Baur, H., Graf, T., Schlu¨chter, C., Signer, P., and Wieler, R.: Dating of Sirius Group tillites in the Antarctic Dry Valleys with cosmogenic3He and21Ne, Earth Planet Sc Lett, 147, 37–54, https://doi.org/10.1016/s0012-821x(97)00003-4, 1997.

Cerling, T.: Geomorphology and In-Situ Cosmogenic Isotopes, Annu Rev Earth Pl Sc, 22, 273–317, https://doi.org/10.1146/annurev.earth.22.1.273, 1994.

Heisinger, B., Lal, D., Jull, A. J. T., Kubik, P., Ivy-Ochs, S., Neumaier, S., Knie, K., Lazarev, V., and Nolte, E.: Production of selected cosmogenic radionuclides by muons 1. Fast muons, Earth Planet Sc Lett, 200, 345–355, https://doi.org/10.1016/s0012-821x(02)00640-4, 2002.

Kasbohm, J. and Schoene, B.: Rapid eruption of the Columbia River flood basalt and correlation with the mid-Miocene climate optimum, Sci Adv, 4, eaat8223, https://doi.org/10.1126/sciadv.aat8223, 2018.

Kracek, F. C. and Newronen, K. J.: Thermochemistry of plagioclase and alkali feldspars. Am J Sci (Bowen Volume), 293:318, 1952.

Larsen, I. J., Farley, K. A., Lamb, M. P., and Pritchard, C. J.: Empirical evidence for cosmogenic 3He production by muons, Earth Planet Sc Lett, 562, 116825, https://doi.org/10.1016/j.epsl.2021.116825, 2021.

Larsen,I.J., Farley,K.A., Lamb, M.P.: Cosmogenic 3He production rate in ilmenite and the redistribution of spallation 3He in fine-grained minerals. Geochimica et cosmochimica acta, 265,19–31. Doi: 10.1016/j.gca.2019.08.025, 2019.

Matsuoka, K., Skoglund, A., Roth, G., Pomereu, J. de, Griffiths, H., Headland, R., Herried, B., Katsumata, K., Brocq, A. L., Licht, K., Morgan, F., Neff, P. D., Ritz, C., Scheinert, M., Tamura, T., Putte, A. V. de, Broeke, M. van den, Deschwanden, A. von, Deschamps-Berger, C., Liefferinge, B. V., Tronstad, S., and Melvær, Y.: Quantarctica, an integrated mapping environment for Antarctica, the Southern Ocean, and sub-Antarctic islands, Environ Modell Softw, 140, 105015, https://doi.org/10.1016/j.envsoft.2021.105015, 2021.

Schäfer, J. M., Ivy-Ochs, S., Wieler, R., Leya, I., Baur, H., Denton, G. H., and Schlüchter, C.: Cosmogenic noble gas studies in the oldest landscape on earth: surface exposure ages of

the Dry Valleys, Antarctica, Earth Planet Sc Lett, 167, 215–226, https://doi.org/10.1016/s0012-821x(99)00029-1, 1999.
Subramaniam, A. P.: Mineralogy and Petrology of the Sittampundi Complex, Salem District, Madras State, India. Geol Soc Am Bull, 67 (3): 317–390. Doi: https://doi.org/10.1130/0016-7606(1956)67[317:MAPOTS]2.0.CO;2, 1956.
United States Geological Survey: Taylor Glacier [map] 1:250,000. USGS 1:250,000 Topographic Reconnaissance Series (Topographic), sheet ST 57-60/5. Reston, VA: The Survey, 1